Laser probing of velocity-subgroup dependent rotational alignment of N 2 + drifted in He

Eric B. Anthony, Wolfgang Schade, Michael J. Bastian, Veronica M. Bierbaum, and Stephen R. Leone

Citation: The Journal of Chemical Physics **106**, 5413 (1997); doi: 10.1063/1.473604
View online: http://dx.doi.org/10.1063/1.473604
View Table of Contents: http://scitation.aip.org/content/aip/journal/jcp/106/13?ver=pdfcov
Published by the AIP Publishing

Laser probing of velocity-subgroup dependent rotational alignment of N_2^+ drifted in He

Eric B. Anthony, Wolfgang Schade,[a] Michael J. Bastian,[b] Veronica M. Bierbaum, and Stephen R. Leone[c]
JILA, National Institute of Standards and Technology, Department of Physics and Department of Chemistry & Biochemistry, University of Colorado, Boulder, Colorado 80309-0440

(Received 7 October 1996; accepted 31 December 1996)

Results are presented for Doppler-resolved laser-induced fluorescence measurements of collision-induced rotational alignment of $N_2^+(v''=0)$ drifted in He in a drift-tube apparatus. A single-frequency ring dye laser is used to probe the $R_1(N''=15)$ rotational line of the $B\ ^2\Sigma_u^+ - X\ ^2\Sigma_g^+$ system both parallel and perpendicular to the drift field at three different field strengths and at several different Doppler-selected velocities. A strong correlation is found between the degree of rotational alignment and the velocity subgroup probed along the field direction. For field strengths of 8 and 16 Td and laser probe parallel to the drift field, there is a monotonic increase in the quadrupole alignment parameter $A_0^{(2)}$ with higher velocity subgroup, up to a maximum value of $A_0^{(2)} = -0.150$ (6) for 16 Td at the high-velocity tail. There is evidence that the correlation between alignment and velocity increases with increasing field strength. The mechanisms of the alignment are discussed and these results are attributed primarily to the change in anisotropy of the relative velocity vector distribution of the N_2^+–He pair with field strength. © *1997 American Institute of Physics.* [S0021-9606(97)02113-2]

I. INTRODUCTION

Collision-induced rotational alignment of neutral diatomics and linear molecules has been studied in supersonic jet expansions by polarized absorption and fluorescence detection techniques. Alignment can be produced when there exist anisotropies both in the interaction potential and the relative velocity vector distribution, the latter caused by velocity slip in the jet expansion. Substantial degrees of alignment are reported, for instance, in sodium dimer expanded in sodium,[1] in I_2 seeded in He, D_2, and H_2,[2] and for the expansion of CO_2 seeded in Ar, He, and H_2.[3] All of these studies find a propensity for the rotational angular momentum vectors of the molecules to be aligned perpendicular to the jet expansion direction, a picture most easily understood by the model first suggested by Gorter,[4] who pointed out that the collisional cross section of a rotating molecule is orientation dependent and, for linear molecules, is minimized for the repulsive part of the interaction potential when the angular momentum vectors are aligned perpendicular to the flow direction. Few rotational alignment experiments have been performed on ion-neutral systems, which have correspondingly longer range and more attractive interaction potentials, or on systems at near-thermal energies, where one would still expect analogues to the velocity slip responsible for bulk alignment in supersonic jets.

The first observation of rotational alignment in an ion–neutral system was reported by Dressler *et al.*[5] using a drift tube apparatus. The N_2^+ $(v''=0)$ ions drifted in He were studied by polarized laser-induced fluorescence (LIF) with a broadband Nd:YAG pumped dye laser. By probing perpendicular to the tube axis, at a drift field corresponding to an average center-of-mass collision energy of 52 meV, Dressler *et al.* measured fully velocity-averaged polarization coefficients for two rotational states, $N''=4$ and $N''=10$. They found a corresponding $A_0^{(2)}$ quadrupole alignment parameter of -0.11 ± 0.05 for both states, the sign and magnitude indicating a significant preference for the rotational angular momentum vectors to be aligned perpendicular to the field direction. This early N_2^+–He drift-tube study subsequently motivated theoretical work by Rosmus, Werner, and colleagues. In a series of three papers, a ground-state *ab initio* N_2^+–He interaction potential surface was calculated,[6] and both quantum close-coupled (CC)[7] and classical-trajectory scattering calculations[8] were performed with this potential surface, using as a framework a steady-state formalism and semiempirical relative velocity vector distribution function developed by Meyer and Leone.[9] This theoretical work produced approximate qualitative but not quantitative agreement with the experimentally determined alignment parameters; specifically, the theoretical CC $A_0^{(2)}$ values were found to be -0.010 and -0.034 for the $N''=4$ and 10 states, respectively, smaller in absolute value than the experimental parameters by factors of 11 and 3.[7] A better agreement could be reached by adjusting the second coefficient of the Legendre moment expansion of the relative velocity vector distribution, underscoring the importance of the precise degree of anisotropy in the distribution of relative velocity vectors as well as in the interaction potential for determining the resultant steady-state alignment.

Although the work of Dressler *et al.*[5] used the nonintru-

[a]Permanent address: Institute for Experimental Physics, University of Kiel, D-24098 Kiel, Germany.
[b]Presently attending Boston College Law School, Boston, MA; electronic mail: bastiami@tony.bc.edu
[c]Staff member, Quantum Physics Division, National Institute of Standards and Technology.

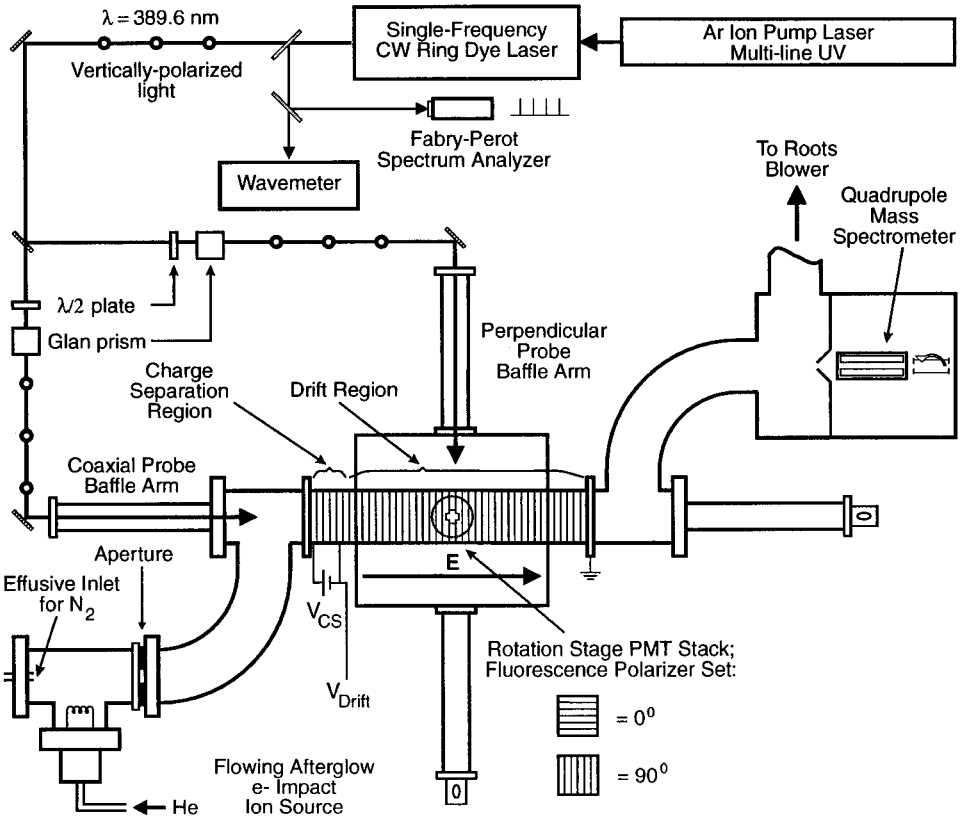

FIG. 1. Overall schematic of flow-drift apparatus, along with the relevant LIF geometry for polarized fluorescence detection.

sive and state-specific technique of laser-induced fluorescence, this first N_2^+–He experiment had several shortcomings. In particular, the low duty cycle of the pulsed dye laser resulted in inherently poor signal-to-noise; to obtain adequate signal, the dye laser had to be run with sufficient power to saturate the transition, introducing further complications to the data analysis.[10] Additionally, the broad linewidth of the pulsed laser (approximately 0.9 cm^{-1}) meant that the experiment was incapable of resolving velocity subgroup alignment, or indeed, any details about the underlying velocity component distribution. It is now possible to resolve velocity subgroup alignment by a cw laser drift-tube experiment with better than 1 MHz resolution that circumvents many of the difficulties in the original experiment. Here, we present results of sub-Doppler alignment determinations of a single high-lying rotational state, $N''=15$, of $N_2^+(v''=0)$ probed by LIF in the $B\ ^2\Sigma_u^+ - X\ ^2\Sigma_g^+$ system at three different field strengths. We find an increase in alignment for increasing field strength and, for a fixed field strength probed along the field direction, a large monotonic increase in the degree of alignment with higher velocity subgroup. The data suggest that the degree of correlation between alignment and velocity increases with increasing field strength. We believe this to be the first observation of velocity-correlated rotational alignment in an ion-neutral system.

II. EXPERIMENT

The technique of single-frequency LIF determination of ion transport properties in a drift-tube apparatus has been described in detail for previous experiments conducted by this group on Ba^+ in He[11] and in Ar,[12,13] and CO^+ in He.[14] A brief overview is given, with emphasis on the details significant for the N_2^+–He rotational alignment work presented here. As in the previous work, a trace amount of N_2^+ is drifted with helium as the buffer gas in a standard flow-drift apparatus; an external axial electric field varies the center-of-mass collision energy of the ion–neutral pair. The net effect of the external field is to establish a steady-state anisotropic ion velocity distribution, the precise character of which is determined by the ion–buffer interaction potential and the field strength. The anisotropies of both the velocity distribution and the potential couple together to produce rotational alignment, the degree of which can in general depend on both rotational state and specific laboratory velocity probed. The major departures from the earlier N_2^+ alignment experiment are the use of a single-frequency cw ring dye laser and the ability to probe both perpendicular and parallel to the drift field. The degree of alignment as a function of a component of sub-Doppler laboratory velocity is measured by single-frequency LIF. A simple scheme is adopted to determine the dominant quadrupole alignment parameter $A_0^{(2)}$as a function of probed velocity; the polarization axis of the probe laser beam is fixed vertically, and the degree of linear polarization of the laser-induced fluorescence is measured by rotating a polarizer so that its transmission axis is either parallel (0°) or perpendicular (90°) to the axis of the drift tube. Sub-Doppler measurements are made for both perpendicular and coaxial laser probe geometries; the perpendicular probe

measurements essentially determine velocity-averaged alignment, while the coaxial probe measurements determine the alignment as a function of the velocity component parallel to the field.

A schematic of the experimental apparatus is shown in Fig. 1. The N_2^+ ions are created 58 cm upstream of the drift region by a flowing afterglow ion source. Helium buffer gas at a typical flow rate of 5.6×10^{21} atoms s^{-1} is passed through two liquid nitrogen cooled cold traps, each containing molecular sieve. The helium buffer then flows over an electron impact ion source configured as an electron gun; the grid voltage is 23 V and the emission current is regulated by a feedback circuit at 1.00 mA. This configuration creates copious metastable He atoms which react with a flow of 1.0×10^{19} molecules s^{-1} of 99.995% purity neutral N_2 introduced into an effusive inlet 7 cm upstream of the ion source. A 2.9-cm-diam aperture in the source region 10 cm downstream of the filament increases the residence time of the gases in the source region to drive the ion chemistry to completion. The major reaction producing $N_2^+(v''=0)$ is Penning ionization of N_2 by $He(2\,^3S)$.[15] Note in particular that the flowing afterglow source produces a thermalized N_2^+ rotational distribution whose angular momentum vectors are isotropically distributed; the rotational alignment is established by subsequent directed collisions with the He buffer gas in the drift region.

The resulting plasma flows through a 44-cm-long field-free flow region to a 45-cm-long drift region, consisting of 1-cm-wide by 7.3-cm-i.d. stainless steel guard rings, electrically insulated by mylar spacers and connected in series by precision 500 Ω resistors. A strong (2.5 V cm^{-1}) electric field across the first five rings of the drift region is used to charge-separate the negative charges (predominantly electrons) from the plasma, resulting in a space-charge limited density of N_2^+ ions in neutral He. We estimate the density of N_2^+ in the drift region as 10^5 cm^{-3}. A variable drift voltage across the remaining 40 guard rings establishes a uniform axial electric field; in a drift tube, the field parameter is the ratio E/N of electric field to buffer gas number density, conventionally measured in townsend (1 Td$=10^{-17}$ V cm^2).[16] For this work, measurements were confined to three field strengths: plasma (both charge separation and drift fields off), 8 Td, and 16 Td. It was found that 16 Td (corresponding to 2.7 V cm^{-1}) was the highest field strength with sufficient signal to perform sub-Doppler polarization measurements. A capacitance manometer is used to measure the pressure in the flow tube, which is held at 0.50 Torr (67 Pa) for all electric fields. A quadrupole mass spectrometer downstream of the drift region is used as a diagnostic for the ion production conditions.

An actively stabilized cw ring dye laser with an effective linewidth of less than 1 MHz is used to probe the ions either perpendicular or parallel (coaxial) to the electric field. We use a proprietary near-UV dye[17] pumped by 4.8 W of multiline UV of an Ar ion laser; 100 mW of single-frequency power can be routinely achieved with fresh dye. The output beam of the ring dye laser is nominally vertically polarized; this polarization is preserved through the beam transport for either perpendicular or coaxial probe by UV-enhanced mirrors. A zero-order polymer half-wave plate and Glan–Taylor polarizing prism are used to compensate for small deviations from true vertical polarization. The laser beam is introduced into the drift tube through baffle arms designed to minimize scattered laser light; each exit baffle arm is terminated by a Brewster-angle window to ensure that no backreflections counterpropagate through the apparatus. Rotational line identifications are made with an external scanning Michelson interferometer wavemeter with an absolute accuracy of ±0.05 cm^{-1}, and laser scan widths are determined from the fringes of a 1.5 GHz confocal Fabry–Perot cavity. The ring dye laser is scanned and positioned in frequency by a microcomputer-controlled digital-to-analog ramp. We pump the $R_1(15)$ rotational line of the (0,0) band in the $B\,^2\Sigma_u^+-X\,^2\Sigma_g^+$ system at 389.6 nm and observe unresolved P and R branch fluorescence of the (0,1) band at 427.8 and 425.6 nm through an 8 nm bandpass interference filter centered at 430 nm; the bandpass of the filter favors transmission of P-branch over R-branch fluorescence by a factor of approximately 9:1 for this rotational line.

The laser-induced fluorescence is imaged by a biconvex lens mounted directly above a fused silica vacuum window and then passes through the bandpass interference filter to a blue-sensitive photomultiplier tube (PMT). The photocathode can be completely shuttered from all fluorescence for a thermionic dark count check. For the sub-Doppler alignment measurements, a 5.1-cm-diam dichroic polarizer with an extinction ratio of better than 10^{-3} is inserted between the lens and interference filter. The entire PMT stack is mounted on a commercial manually driven rotation stage, which permits the transmission axis of the fluorescence polarizer to be set to any continuously adjustable angle. Measurements were largely confined to 0° and 90°, although a small number of diagnostic trials at other angles were performed.

The fluorescence PMT signal is processed by standard photon counting techniques and sent to a 16-bit microcomputer-controlled counter. An instantaneous measure of ring dye laser power, derived from the normalizing photocell of the laser's cavity side-lock system was amplified and sent to a voltage-to-frequency converter whose output in turn was sent to a second counter. Sub-Doppler polarization data collection consists of a sequence of hardware-gated counting trials, varying from 8 to 20 s in length. A precision crystal-locked trial gate is fed to the counters for LIF and laser power. Periodic sampling at either 0.5 or 1 s intervals allowed determination of the average counting rate in the interval and the spread in these counting rates. Trials are performed at discrete and well-defined sub-Doppler positions, as determined by a 7.65 GHz unpolarized LIF calibration scan taken immediately prior to the trials. For perpendicular probe, sub-Doppler polarization data were taken at three different positions across the profile, while five points were taken for coaxial probe. The trial sequences are interleaved so that these sub-Doppler points are taken close together in time.

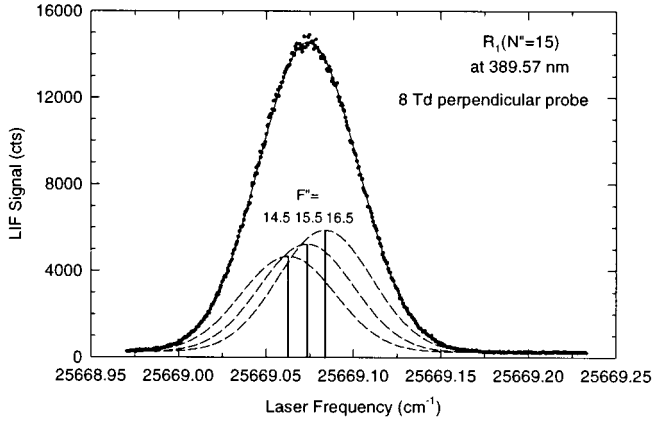

FIG. 2. Typical LIF spectrum of $R_1(15)$ at 8 Td. Approximate underlying hyperfine component spacings and isotropic intensities are shown in the stick spectra.

III. RESULTS

Typical LIF data for the $R_1(N''=15)$ line at 8 Td probed perpendicular to the field are shown in Fig. 2. As indicated in the figure, there are unresolved Doppler-broadened hyperfine components underlying each of the spin–rotation branches. Although the general spectroscopic structure of the $B\ ^2\Sigma_u^+ - X\ ^2\Sigma_g^+$ system is well-known,[18–20] and the energy spacing of these hyperfine components has been well-studied for the $(v',v'')=(0,1)$[21] and $(1,2)$[22] bands of $^{14}N_2^+$ by the technique of fast ion-beam laser spectroscopy, it appears that precise spectroscopic magnetic hyperfine parameters for $v''=0$ have not previously been calculated or measured with a sub-Doppler resolution experiment. A simple linear extrapolation of the known b_F'' and t'' coupling constants[20] for $v''=2$ and 1 gives a $v''=0$ hyperfine component spacing of approximately 0.01 cm^{-1} (0.3 GHz). However, here we use the measured $v''=1$ spacings[21] and isotropic line strengths, even though these values are slightly too large, as discussed further below. Since the natural linewidth of these transitions is less than 3 MHz,[23] each component can be fit to a good approximation with a symmetric Gaussian line shape. The composite best-fit line shape is shown in the figure, as determined by a four-parameter fit (constant background, overall scaling of the three component Gaussians, overall placement of the stick spectra within the line shape, and the shared width of the three components).

In practice, we have found that such a composite fit is virtually indistinguishable from a simple four-parameter Gaussian fit to the *entire* line shape; since there is currently no accurate hyperfine spectroscopy, all data for this study were analyzed by this latter method. Indeed, a convenient assumption at this level of treatment is to ignore the underlying hyperfine structure entirely and treat the measured line profile as a pure Doppler velocity component distribution due to a single J'' state. The choice of the particular rotor state studied here was motivated by several considerations. The vector model[24] suggests that, for a high-rotor state, both the velocity distributions and rotational alignments of the underlying unresolved F'' states will be essentially the same, since the addition of a vector of fixed length I to $\mathbf{J}$ becomes a perturbation of decreasing importance with increasing J-value. As would be anticipated from this model, the hyperfine depolarization correction factors $\overline{g^{(k)}}$ approach unity rapidly with increasing J;[25] for the state used here, the quadrupole correction factor $\overline{g^{(2)}}$ used below to correct our observed $A_0^{(2)}$ parameters is 0.984. Additionally, although the even N'' rotational lines are twice as intense, they are associated with six (five distinct) hyperfine components, while the odd N'' lines have only three nonoverlapping components.[20] For this study, we choose the highest-lying odd-N'' state acces- sible with good signal-to-noise, which is $R_1(N''=15)$ $(J''=15.5)$. This is the highest rotational line in the R-branch with reasonable signal at all field strengths, and, despite the Doppler broadening with increasing field strength, this line remains well-separated from its neighboring spin doublet $R_2(15)$. In short, this single-J'' approximation is justifiable because of the small degree of spin depolarization and closeness of spacing of the underlying hyperfine structure and is appropriate for the relatively coarse sampling of velocity components in this work.

For the sub-Doppler polarization trials, the raw data consist of a total number of counts accumulated by the LIF signal counter for a particular trial lasting from 8 to 20 s, at a particular laser frequency and polarizer setting. Typical total counting rates for 8 Td at line center are 7300 counts s^{-1} or greater for coaxial probe. Each trial must be corrected for background and ring dye laser power fluctuations. An effective background measurement is made for each polarizer setting of each sequence by tuning the laser approximately 3.7 GHz or more away from the line center and accumulating background counts for an interval of time equal to the LIF trial interval. This background is then subtracted from the total counts accumulated during the LIF trial. The three major components of this effective background are residual scattered laser light, flowing afterglow fluorescence, and PMT dark counts, the latter being the dominant background contributor at typically 200 counts s^{-1}. Scattered laser light contributions are held to typically less than 120 counts s^{-1} for perpendicular probe and 20 counts s^{-1} for coaxial probe by careful beam transport aided by two prealigned counterpropagating HeNe lasers. Flowing afterglow fluorescence is quenched by the neutral N_2 flow to typically 40 counts s^{-1} or less. After background subtraction, the ring dye laser power dependence of the resulting LIF signal is corrected by simple division by the accumulated trial counts in the laser power channel, since the LIF signal under these production conditions remained linear with laser power up to the maximum of 50 mW of power at the baffle arm entrances. A conventional linear polarization coefficient is then calculated from the background and laser-power corrected LIF signals as

$$P(\chi_a=90°)=\frac{I_{0°}-I_{90°}}{I_{0°}+I_{90°}}, \tag{1}$$

where χ_a is the laser polarization angle ($\chi_a = 90°$ is vertically polarized light). Uncorrected polarization coefficients, as directly calculated by this procedure, are obtained for both

TABLE I. (a) Perpendicular probe results.[a] (b) Coaxial probe results.[a]

Field (Td)	Frequency marker (Fig. 3)	No. of observations	Detuning (GHz)[b]	Uncorrected[c] $P(90°)\times100\%$	Corrected[d] $P(90°)\times100\%$	Alignment parameter $A_0^{(2)}$
			(a)			
(Plasma)	1	8	−0.95	+3.0±0.2	+0.0±0.4	+0.001(7)
(Plasma)	2	8	+0.00	+3.0±0.1	+0.0±0.3	+0.000(7)
(Plasma)	3	8	+0.95	+3.1±0.5	+0.1±0.6	−0.001(11)
8	1	10	−0.68	+4.5±0.3	+1.0±0.3	−0.019(7)
8	2	10	+0.30	+4.5±0.1	+0.9±0.3	−0.019(5)
8	3	10	+1.28	+4.6±0.3	+1.0±0.4	−0.021(8)
16	1	8	−1.11	+4.8±0.3	+1.8±0.4	−0.036(8)
16	2	8	+0.00	+4.7±0.2	+1.7±0.4	−0.035(8)
16	3	8	+1.11	+4.9±0.2	+1.9±0.4	−0.038(7)
			(b)			
(Plasma)	1	15	−1.42	−3.5±0.1	+0.1±0.2	−0.002(3)
(Plasma)	2	16	−0.94	−3.6±0.1	+0.0±0.2	+0.001(3)
(Plasma)	3	15	+0.01	−3.4±0.1	+0.2±0.2	−0.003(3)
(Plasma)	4	16	+0.97	−3.6±0.2	−0.1±0.2	+0.001(4)
(Plasma)	5	16	+1.45	−3.6±0.2	−0.1±0.3	+0.001(5)
8	1	12	−1.46	−3.5±0.2	+0.1±0.2	−0.002(4)
8	2	12	−0.97	−2.6±0.1	+1.0±0.2	−0.020(3)
8	3	12	+0.03	−0.9±0.1	+2.6±0.2	−0.053(3)
8	4	12	+1.03	+0.7±0.2	+4.2±0.3	−0.085(5)
8	5	12	+1.53	+1.4±0.3	+5.0±0.3	−0.100(6)
16	1	12	−1.60	−3.6±0.2	−0.1±0.2	+0.001(4)
16	2	12	−1.04	−2.2±0.1	+1.4±0.2	−0.028(3)
16	3	12	+0.06	+0.2±0.1	+3.8±0.2	−0.076(3)
16	4	12	+1.16	+3.0±0.2	+6.5±0.2	−0.130(3)
16	5	12	+1.72	+4.0±0.3	+7.5±0.3	−0.150(6)

[a]All error bars represent one standard deviation of the mean and reflect statistical error only.
[b]Detuning from line center at this field strength, all ±0.02 GHz.
[c]Background and laser-power corrections only.
[d]With systematic corrections, as discussed in the text.

perpendicular and coaxial probe for three field conditions: plasma (all fields off), 8 Td, and 16 Td and presented in Tables I(a) and I(b); the systematic offsets in this data are discussed below.

An important systematic check for either probe geometry is performed by recording sub-Doppler measurements with both the charge-separation and drift fields off. The N_2^+ molecules in the resulting plasma experience no field and therefore their velocity distribution should be strictly Maxwell–Boltzmann, with a resulting linewidth characterized by the temperature of the buffer gas. The relative velocity vector **g** of the N_2^+–He pair is then isotropically distributed and no alignment is possible. In principle, all zero-field $P(90°)$'s for either probe geometry and at any laser frequency should vanish. However, the measurements are not free of spurious polarization, which results in nonzero fluorescence polarization coefficients even in the complete absence of molecular alignment. For this work, spurious polarization acts as the major systematic error that affects the accuracy of the alignment parameters calculated from the measured polarization coefficients.

The uncorrected plasma polarization coefficients in Table I indicate that there are different spurious polarization systematics for each probe geometry; a more extensive set of diagnostic measurements was performed for coaxial than for perpendicular probe. One check involved removing the polarizer from the PMT stack and performing 0°/90° stack rotations for coaxial probe as if polarization coefficients were being measured. Comparison of these ''polarization'' measurements with true polarization measurements taken by locking the PMT stack to one position and manually rotating just the polarizer indicates that the rotation of the entire PMT stack introduces a small degree of variation, which we believe is primarily due to small geometrical modulations of the effective detector solid angle as the PMT stack rotations are performed. Coaxial ''polarization'' measurements taken of the plasma at line center with no polarizer in the stack yield a coefficient x 100% of -1.59 ± 0.07. We calculate from each pair of these 0°/90° isotropic measurements a geometrical correction factor f,

$$f=\frac{I_{0°\ \text{measured isotropic}}}{I_{90°\ \text{measured isotropic}}}=0.969\pm0.004, \tag{2}$$

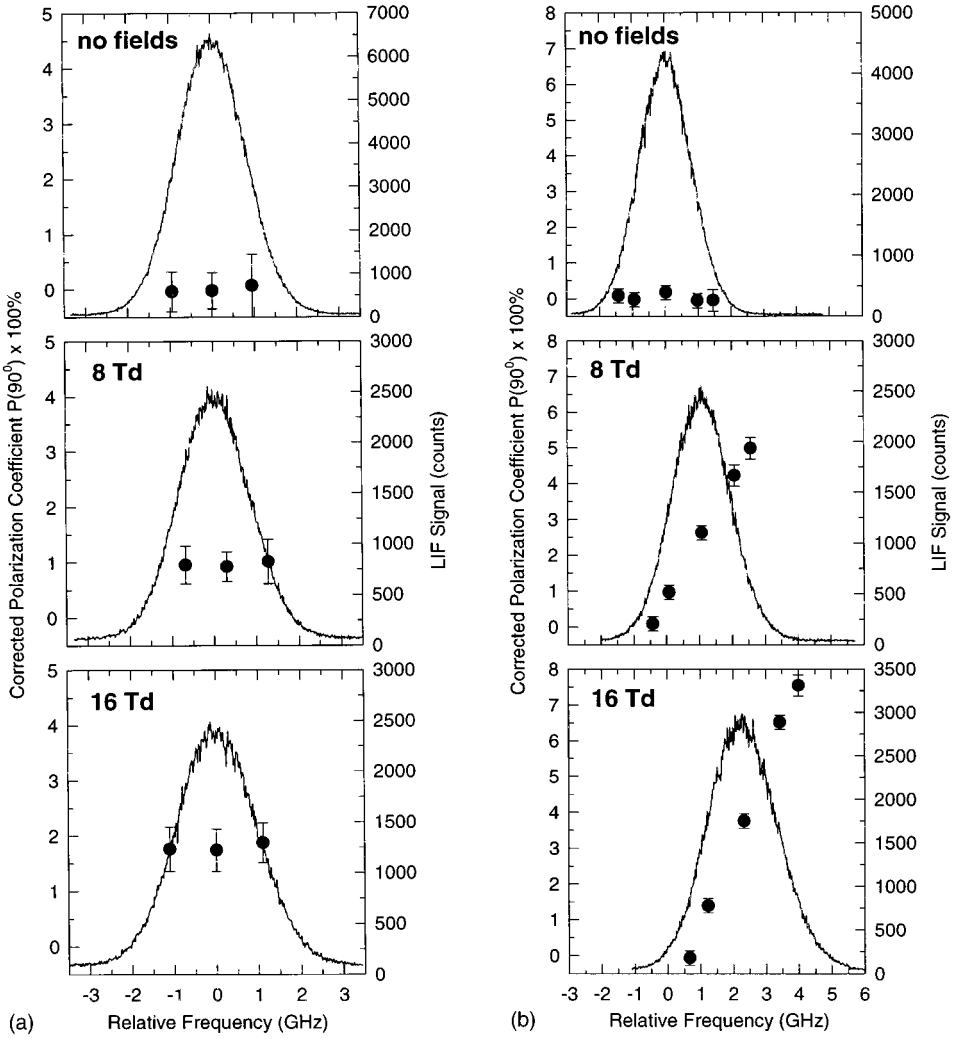

FIG. 3. (a) Perpendicular probe and (b) coaxial probe alignment results for three different field strengths. Corrected polarization coefficients, with the corrections discussed in the text, are plotted at the laser detunings at which they were acquired. Frequency markers in Table I are numbered from left to right.

which can then be used to multiplicatively correct the 90° background and laser-power corrected LIF intensities for the actual polarization measurements as

$$P(90°)_{f\text{-corrected}} = \frac{I_{0° \text{ measured}} - fI_{90° \text{ measured}}}{I_{0° \text{ measured}} + fI_{90° \text{ measured}}}. \tag{3}$$

However, it appears there is an additional unidentified source of spurious polarization. Coaxial probe plasma measurements made with the rotation stage locked at 0° and just the polarizer itself manually rotated to 0°/90° yield a polarization coefficient x 100% of -1.98 ± 0.07; this indicates that the geometrical modulation is not the only systematic present. We believe that the measured plasma LIF is not totally unpolarized, and we subtract this offset from the f-corrected polarizations to obtain a set of corrected polarizations as listed in Table I.

There are several possible sources of this additional spurious polarization. If the (vertical) polarization vector of the probe laser beam is not matched exactly to the vertical of the PMT stack, the measured polarization coefficients would not be true $P(90°)$'s. With the current arrangement, it is difficult to assess the matching of the verticals; we estimate the accuracy of the angles as $\pm5°$. Additionally, the wave plate and Glan prism were not used in all measurements, possibly introducing further small deviations from true vertical. It is also possible that the laser entrance windows are slightly birefringent and produce a small degree of elliptically polarized light within the drift tube.[26] The direction and magnitude of the offset spurious polarization is consistent with all of these possibilities. By deliberately rotating the laser polarization angle χ_a to 0°, $P(0°)$'s were also measured for plasma conditions for both perpendicular and coaxial probe. Percentage polarizations of $+14.6\pm0.2$ and -14.9 ± 0.1, respectively, were obtained, in good agreement with the expected theoretical values of $\pm14.3\%$; we are presently unable to account completely for the poorer theoretical agreement of the measured isotropic $P(90°)$'s.

Table I lists both the uncorrected (''raw'') polarization coefficients and the best estimate of the true degree of fluorescence polarization with the corrections discussed above;

TABLE II. Drift velocities and perpendicular and parallel translational temperatures.[a]

Field (Td)	Drift velocities (m/s)	Uncorrected[b] $T_\perp$ (K)	Corrected[c] $T_\perp$(K)	Uncorrected[b] $T_\parallel$ (K)	Corrected[c] $T_\parallel$ (K)
(Plasma)	(0)	330±7	318±8	323±7	312±8
4	180±12	347±7	336±8	349±7	338±8
8	407±15	356±6	345±7	401±6	389±7
16	884±25	443±6	432±7	565±6	554±7

[a]All error bars represent one standard deviation of the mean and reflect statistical error only.
[b]As obtained by fit of line profile to single Gaussian.
[c]Corrected for underlying hyperfine structure, using known $v''=1$ spacings.

the corrected polarization coefficients for perpendicular and coaxial probe are plotted in Figs. 3(a) and 3(b) at the laser detunings at which they were acquired. For coaxial probe at 16 Td, the polarizations vary from essentially 0% in the low velocity tail to +7.5% in the high velocity tail. Note also that the coaxial probe low velocity tail data are unpolarized for each field strength. We stress that all data presented here were taken with an identical PMT stack configuration and under identical experimental conditions. In short, we are confident we are measuring definite *relative* changes in velocity subgroup polarizations across the Doppler profile and can attribute these relative changes to changes in the underlying alignment of N_2^+. We are less confident at present of the *absolute* values of the alignment moments due to the corrections for systematics as discussed above.

For comparison with other experiments and with theory, we convert our polarizations into alignment parameters. The basic theory of detection and characterization of molecular alignment via LIF has been presented in detail in two papers by Greene and Zare.[27,28] In a 1+1 axially symmetric LIF experiment, only two parameters are obtainable: $A_0^{(2)}$ and $A_0^{(4)}$, the quadrupole and hexadecapole alignment parameters, respectively. These parameters correspond to the first two nonisotropic terms of the state multipole expansion of the density matrix ρ^j_{mm}, the diagonal elements of which give the probability of finding an ion in state $|jm\rangle$.[29,30] Here, the corresponding quadrupole alignment parameters for each corrected polarization coefficient are found with the approximation that the hexadecapole moment is negligible. One expects, both on physical grounds for this high-rotor state and from the previous calculations of Follmeg *et al.*,[7] that the dominant parameter is $A_0^{(2)}$ by an order of magnitude or more, so we believe this approximation is not a serious shortcoming for the present results. With this approximation and the chosen measurement scheme, the linear polarization coefficients then have a very simple interpretation: a true $P(90°)$ of zero indicates no rotational alignment, while positive (negative) polarization coefficients are associated with negative (positive) quadrupole alignment parameters, which in turn indicate a preference for the rotational angular momentum vectors to be aligned perpendicular (parallel) to the field axis. As mentioned above, it is necessary to correct the observed alignment parameters for spin depolarization.[25,27,28] The presence of the nonspatial angular momentum vectors associated with the unpaired electronic spin **S** and the coupled nuclear spins **I** leads to a degradation of the degree of observed alignment of the total orbital angular momentum **N**. Here, we correct for the depolarization of the nuclear spins only with the correction factor $\overline{g^{(2)}} = 0.984$ to obtain the true alignment of **J**; note that this correction is essentially negligible at the level of detail of these current measurements. The resulting spin-corrected alignment parameters are tabulated in Tables I(a) and I(b).

Approximate transport property information can also be extracted from the unpolarized LIF calibration data. Drift velocities may be determined from the shift of the first moment of the coaxial LIF line profiles, while translational temperatures may be determined from the width or second central moment of the profiles; the analysis for extracting transport properties from LIF spectra is discussed in detail by Bastian *et al.*[13] for atomic systems. Because of the unresolved hyperfine structure, the observed line shapes are not true Doppler profiles, so translational temperatures obtained directly from these linewidths will be systematically high. However, by using the known $v''=1$ spectroscopy and isotropic line strengths, and assuming the underlying line shapes can be fit to a symmetric Gaussian, we can extract corrected perpendicular and parallel translational temperatures from the observed linewidths. In Table II, approximate drift velocities and translational temperatures are listed. Both uncorrected ''temperatures'' obtained from fitting a single symmetric Gaussian to the line shape and approximate corrected translational temperatures are given. The perpendicular temperatures are additionally broadened because the solid angle of detection includes off-axis ion velocities, which are distributed parabolically in the drift tube.[31] However, the corrected plasma parallel temperature is still about 10 K greater than room temperature, a systematic that we presently cannot account for.

Although, as mentioned above, a fluorescence signal versus laser power check was performed, rough numerical estimates of the photon absorption cross section and photon flux densities on the drift-tube axis suggest that the LIF transition might be partially saturated.[32] However, the estimated degree of saturation (S parameter$\approx$10)[33] cannot account for the systematically high zero-field temperatures. Since the natural linewidth of the transition is less than 3 MHz, the degree of saturation would have to be much greater before any saturation broadening would be detectable in the Doppler linewidths. Additionally, partial saturation would tend to *decrease* the observed polarizations, so that the polarization measurements would slightly underestimate the actual de-

gree of alignment.[34] The spurious polarizations in our measurements cannot be accounted for by saturation. In summary, possible partial saturation would make no qualitative or quantitative difference within the systematic error bars of these measurements.

We can compare these transport property values to the ones used previously by Meyer and Leone[9] to estimate the form of the relative velocity vector distribution. There, it was assumed that the perpendicular temperature was that of the buffer gas, and the parallel temperature was equal to the rotational temperature. Specifically, for 14 Td, it was assumed that $T_\perp = T_{\text{buff}} = 298$ K, and $T_\parallel = T_{\text{rot}} = 405$ K; the drift velocity was taken to be 790 m s^{-1}. This drift velocity is in reasonable agreement with the LIF results, but it is clear from Table II that both of the estimated temperatures are significantly lower by at least 100 K than what is found here.

IV. DISCUSSION

The collision-induced rotational alignment observed in this experiment is a product of anisotropies in both the ion–neutral interaction potential and relative velocity vector distribution, appropriately modified by the partial velocity selection imposed by the single-frequency laser. However, correlations between velocity subgroups and their degree of rotational alignment have not been demonstrated experimentally until quite recently. Aquilanti and co-workers have, in a supersonic jet expansion coupled to a molecular beam and Stern–Gerlach apparatus, found a dramatic change in the degree of rotational alignment of neutral O_2 mixed with various carrier gases.[35] In the most extreme case of O_2 expanded in He, the polarization varied from essentially zero in the low velocity tail of the beam to greater than 80% in the high-velocity tail. The formal similarity between the plots of their data and Fig. 3(b) is striking. Aquilanti *et al.* ascribe their results to a large number of intermediate impact-parameter collisions that both accelerate and reorient the molecules, leading to the observed high degree of correlation between beam velocities and alignment.

It is quite possible that the rotational alignment observed in the present experiment proceeds by a similar mechanism. The alignment observed in both experiments is created by many hundreds of collisions over the whole range of impact parameters. Aquilanti *et al.*[35] find essentially no alignment in the low-velocity tail of their distributions, which appears to be the case here as well. It is quite possible that there is a narrow range of impact parameters that leads to both small-angle forward scattering and considerable rotational alignment, which would account for the correlation between velocity subgroups and alignment. Additionally, although the N_2^+–He complex possesses a well approximately 140 cm^{-1} deep, it is unlikely that the observed alignment proceeds by a collision complex. For the high rotor state chosen for this work, adjacent rotor levels accessible by the $\Delta j = \pm 2$ collisional selection rule for homonuclear diatomics lie about 120 cm^{-1} apart, which suggests that rotationally elastic scattering predominates. It can be shown that in the limiting case of purely elastic scattering via a long-lived collision complex, no net alignment would result.[2]

The single-frequency cw laser technique used in this experiment measures velocity vector projections along the laser propagation direction **k**; ions that have laboratory velocity components along **k** in resonance with the laser frequency can absorb a photon and fluoresce. The result of probing in a particular direction is a steady-state velocity component distribution function, which is a projection of the *complete* ion velocity distribution function.[12,13] If we assume that the components of the complete velocity distribution function are either uncorrelated or very weakly correlated and thus separable, the perpendicular and coaxial probe data provide two orthogonal ''slices'' of this distribution function. Probing perpendicular (parallel) to the drift-tube axis at a particular frequency effectively constrains the laboratory component of the fluorescing molecules along **k**, while the component orthogonal to **k** can range freely over all possible values with a distribution given by the parallel (perpendicular) velocity component distribution. Thus a specific probe direction gives an effective average over the other, orthogonal direction.

There are several significant qualitative features to be explained in the present data. For perpendicular probe at a fixed field strength, the polarization coefficients are essentially equal across the Doppler profile and the degree of polarization increases with increasing field strength. For coaxial probe at a fixed, nonzero field strength, the degree of polarization increases monotonically across the Doppler profile, and the slope of this increase appears to increase as well with field strength, as can be seen in Fig. 3(b). Additionally, inspection of Fig. 3 will reveal that data points taken at the same laser detuning (i.e., absolute frequency) but at different field strengths do not in general have the same alignment.

A simple qualitative explanation of these features is possible. The anisotropy of the relative velocity vector distribution is most pronounced in the field direction. The perpendicular probe polarizations always average over these anisotropies. If the velocity distribution function is separable, these data will then be insensitive to the particular velocity vector component selected by the laser and will be an effective average over the field direction. This would imply no variation across the Doppler profile for perpendicular probe and a fixed field strength; as the field strength is increased, the field direction anisotropy increases, and the perpendicular polarizations increase as well. Likewise, the coaxial probe polarizations average over the radial or perpendicular velocity components, but now each data point represents a velocity slice taken along the direction of greatest anisotropy. For a fixed field strength, as the laser is scanned from the low to the high-velocity tail of a coaxial Doppler profile, the relative velocity vector distribution becomes increasingly more directed, as reflected by the increasing coaxial polarizations with increasing laser frequency. Again, the degree of anisotropy increases with increasing field strength, so the slope of the polarizations will increase. The polarizations of data points taken at the same laser frequency but at different field strengths will in general not be equal. Although these points have in common the scalar magnitude of the velocity com-

ponent v_l selected out by the laser, these slices are drawn from different velocity distribution functions with different vector properties; the alignment is not solely dependent on this scalar component. Note in particular that if the observed alignment did somehow depend on the magnitude of v_l alone, then it would be possible to observe alignment in the high- or low-velocity tail of a zero-field Doppler profile, contrary to both intuition and experimental evidence.

An indirect comparison of this data with the earlier experiment is also possible. From the above arguments, one would expect the perpendicular probe alignment at a particular field strength to be the coaxial probe velocity-averaged result (i.e., the coaxial alignment at line center). However, there is rather poor agreement between the values of the perpendicular probe alignment parameters at 8 and 16 Td [$A_0^{(2)} = -0.019(5)$ and $-0.035(8)$, respectively] and the corresponding coaxial probe values at line center [$A_0^{(2)} = -0.053(3)$ and $-0.076(3)$]. We believe this is primarily due to uncorrected systematics still present in the perpendicular data; the coaxial probe alignment data were obtained with more effort and thus we believe these moments are more accurate. An indirect comparison can then be made of this 16 Td coaxial quadrupole parameter at line center for $N'' = 15$, $A_0^{(2)} = -0.076$, with the broadband perpendicular probe alignment, $A_0^{(2)} = -0.11$, obtained in the earlier Dressler *et al.* experiment at 14 Td on $N'' = 10$. Even with possible unresolved systematics, it appears certain that the fully velocity-averaged alignments measured here are smaller in absolute value than what was found in the original experiment, and closer to theoretical dynamic calculations.[7,8]

Both because of possible unresolved systematics and because Follmeg *et al.* performed fully velocity-averaged calculations for significantly lower rotor states, a detailed or quantitative comparison of experiment with theory is not addressed at present. Qualitatively, the measured alignment parameters depend on products of the Legendre moment expansion coefficients of both the relative velocity vector distribution and the alignment or tensor cross sections, integrated over all relative speeds g.[36] The single-frequency laser used in this experiment imposes a degree of partial velocity selection that modifies this dependence. The net effect of fully resolving one laboratory velocity component is to introduce a quasi-Gaussian function $F(g;v_l)$ into this integral; this function represents the ''narrowing'' and tunable element in relative speed space introduced by probing in a specific direction with a single-frequency laser.[37,38] Although the precise form of this function depends on the direction probed, in general, for $v_l > \sqrt{k_B T/\mu}$, $F(g;v_l)$ is peaked at approximately v_l, and has a width that scales approximately as $\sqrt{v_l^2 + (k_B T/\mu)}$. This narrowing function will multiply both the tensor cross sections and the relative velocity vector distributions in a convolution integral. The tensor cross sections contain all the information about the anisotropies in the attractive and repulsive parts of the N_2^+–He interaction potential as a function of relative speed. However, we believe that the qualitative features of this data discussed above and exhibited in Fig. 3 are primarily due to the changes in the anisotropy of the relative velocity vector distribution as $F(g;v_l)$ is tuned around in relative speed space within these integrals. This is reasonable considering that, at thermal energies, the repulsive part of the potential is primarily sampled, while the change in anisotropy of the velocity distribution is large over the range of component velocities selected out by the laser. In summary, we believe the anisotropies of the relative velocity vector distribution will dominate the general character of the measurements. The effect of the interaction potential is a secondary consideration at the level of accuracy of the present data; the precise dependence of the tensor cross sections on relative speed will determine the particular values of the observed alignment.

V. CONCLUSION

Preliminary results have been presented for the determination of rotational alignment for a single rotational line of N_2^+ via LIF in the N_2^+–He system as a function of a laser-selected velocity component in a drift-tube experiment. In general, two additional pieces of information have been obtained beyond the earlier N_2^+–He experiment. For one, it has been shown, both theoretically[7,8] and here experimentally, that the degree of alignment is quite sensitive to the form of the complete relative velocity vector distribution. Previously, the parameters that determined this form had to be estimated or guessed at. However, with the current experiment, the transport properties can be measured more-or-less directly as a function of rotational state and field strength; these in turn determine the precise form of the vector distribution. With accurate $v''=0$ hyperfine spacings, which could be calculated from *ab initio* Hartree–Fock–Roothaan wave functions, as was done by Rosner *et al.*[39] for the computation of $v''=1$ parameters, the Doppler spectra could be fit directly to obtain quite accurate transport property data.

Second, as discussed above, the use of a tunable single-frequency laser introduces a selection element in relative speed space; the tunability of this function over a fairly wide range of relative energies allows one, in principle, to more accurately map out the structure of the underlying tensor cross sections. The Hibridon quantum CC code of Alexander, Manolopoulos, Werner *et al.* used for the original calculations of Follmeg *et al.*[7] has recently been placed in the public domain, which opens up the possibility of additional theoretical work specifically addressing experimentally obtained partially velocity-averaged alignments.[40] An extended set of calculations that addresses higher as well as lower rotor states, in conjunction with more accurate and extensive experimental work, would permit a comprehensive test of an *ab initio* potential and scattering theory against experiment.

ACKNOWLEDGMENTS

E.B.A. wishes to thank Chris Greene, Paul Kleiber, David Nesbitt, Robert Parson, and Sean Casey for many helpful ideas and discussions. W.S. is grateful to the Deutsche Forschungsgemeinschaft for a fellowship. This work was supported by a grant from the Air Force Office of Scientific Research.

[1] M. P. Sinha, C. D. Caldwell, and R. N. Zare, J. Chem. Phys. **61**, 491 (1974).
[2] D. P. Pullman, B. Friedrich, and D. R. Herschbach, J. Chem. Phys. **93**, 3224 (1990); B. Friedrich, D. P. Pullman, and D. R. Herschbach, J. Phys. Chem. **95**, 8118 (1991); D. Pullman, B. Friedrich, and D. Herschbach, *ibid.* **99**, 7407 (1995).
[3] M. J. Weida and D. J. Nesbitt, J. Chem. Phys. **100**, 6372 (1994).
[4] C. J. Gorter, Naturwissenschaften **26**, 140 (1938).
[5] R. A. Dressler, H. Meyer, and S. R. Leone, J. Chem. Phys. **87**, 6029 (1987).
[6] S. Miller, J. Tennyson, B. Follmeg, P. Rosmus, and H.-J. Werner, J. Chem. Phys. **89**, 2178 (1988).
[7] B. Follmeg, P. Rosmus, and H.-J. Werner, J. Chem. Phys. **93**, 4687 (1990).
[8] B. Follmeg, H.-J. Werner, and P. Rosmus, J. Chem. Phys. **95**, 979 (1991).
[9] H. Meyer and S. R. Leone, Mol. Phys. **63**, 705 (1988).
[10] H. Meyer and S. R. Leone, J. Chem. Phys. (in press).
[11] R. A. Dressler, J. P. M. Beijers, H. Meyer, S. M. Penn, V. M. Bierbaum, and S. R. Leone, J. Chem. Phys. **89**, 4707 (1988).
[12] S. M. Penn, J. P. M. Beijers, R. A. Dressler, V. M. Bierbaum, and S. R. Leone, J. Chem. Phys. **93**, 5118 (1990).
[13] M. J. Bastian, C. P. Lauenstein, V. M. Bierbaum, and S. R. Leone, J. Chem. Phys. **98**, 9496 (1993).
[14] C. P. Lauenstein, M. J. Bastian, V. M. Bierbaum, S. M. Penn, and S. R. Leone, J. Chem. Phys. **94**, 7810 (1991).
[15] A. L. Schmeltekopf and F. C. Fehsenfeld, J. Chem. Phys. **53**, 3173 (1970).
[16] E. A. Mason and E. W. McDaniel, *Transport Properties of Ions in Gases* (Wiley, New York, 1988).
[17] F. P. Tully and J. L. Durant, Jr., Appl. Opt. **27**, 2096 (1988). This dye, Exalite 392E, is available from Exciton Chemical Company, Dayton, OH, (513) 252-2989.
[18] A. Lofthus and P. H. Krupenie, J. Phys. Chem. Ref. Data **6**, 113 (1977).
[19] C. H. Townes and A. L. Schawlow, *Microwave Spectroscopy* (McGraw-Hill, New York, 1955).
[20] S. D. Rosner, T. D. Gaily, and R. A. Holt, J. Mol. Spectrosc. **109**, 73 (1985).
[21] T. J. Scholl, A. W. Taylor, R. A. Holt, and S. D. Rosner, J. Mol. Spectrosc. **152**, 398 (1992).
[22] K. Boudjarane, J. Lacoursiere, and M. Larzilliere, J. Chem. Phys. **101**, 10 274 (1994).
[23] T. Fukuchi, A. Y. Wong, and R. F. Wuerker, J. Appl. Phys. **77**, 4899 (1995).
[24] R. N. Zare, *Angular Momentum: Understanding Spatial Aspects in Chemistry and Physics* (Wiley-Interscience, New York, 1988).
[25] J. A. Guest, M. A. O'Halloran, and R. N. Zare, Chem. Phys. Lett. **103**, 261 (1984).
[26] S. Williams (private communication).
[27] C. H. Greene and R. N. Zare, Annu. Rev. Phys. Chem. **33**, 119 (1982).
[28] C. H. Greene and R. N. Zare, J. Chem. Phys. **78**, 6741 (1983).
[29] K. Blum, *Density Matrix, Theory and Applications* (Plenum, New York, 1981).
[30] A. J. Orr-Ewing and R. N. Zare, Annu. Rev. Phys. Chem. **45**, 315 (1994).
[31] E. E. Ferguson, F. C. Fehsenfeld, and A. L. Schmeltekopf, Adv. At. Mol. Phys. **5**, 1 (1969).
[32] D. Nesbitt (private communication).
[33] W. Demtroder, *Laser Spectroscopy*, 2nd corrected printing (Springer, New York, 1982).
[34] R. Altkorn and R. N. Zare, Annu. Rev. Phys. Chem. **35**, 265 (1984).
[35] V. Aquilanti, D. Ascenzi, D. Cappelletti, and F. Pirani, Nature (London) **371**, 399 (1994); J. Phys. Chem. **99**, 13 620 (1995); V. Aquilanti, D. Ascenzi, D. Cappelletti, S. Franceschini, and F. Pirani, Phys. Rev. Lett. **74**, 2929 (1995); V. Aquilanti, L. Beneventi, G. Grossi, and F. Vecchiocattivi, J. Chem. Phys. **89**, 751 (1988).
[36] R. Parson (private communication).
[37] N. Smith, T. A. Brunner, and D. E. Pritchard, J. Chem. Phys. **74**, 467 (1981).
[38] H. Meyer, E. B. Anthony, and S. R. Leone (unpublished).
[39] S. D. Rosner, T. D. Gaily, and R. A. Holt, Phys. Rev. A **26**, 697 (1982).
[40] M. Alexander (private communication).